

Study within the Mining Effects Knowledge Program (KEM-39) on the cyclic storage of gases in the Netherlands

## **WP6: Evaluation of generic guidelines for a safe operational bandwidth of CO<sub>2</sub>, N<sub>2</sub> and H<sub>2</sub> storages in depleted gas fields**

### Authors:

Eng. Isotton Giovanni<sup>1</sup>  
Prof. Janna Carlo<sup>1</sup>  
Prof. Teatini Pietro<sup>1</sup>  
Prof. Deangeli Chiara<sup>2</sup>  
Prof. Rocca Vera<sup>2</sup>  
Prof. Verga Francesca<sup>2</sup>  
Prof. Collettini Cristiano<sup>3</sup>

### Affiliations:

<sup>1</sup>M3E srl  
<sup>2</sup>Politecnico di Torino  
<sup>3</sup>Università la Sapienza

**Document type:** Technical report

**Date:** December 2022

## INDEX

Project Executive Summary .....	3
Introduction.....	5
1 Scenario Comparison.....	6
2 Final observations.....	17
3 Answers to the questions behind the KEM-39 project.....	18
References.....	19

## Project Executive Summary

The KEM-39 project is composed by six work packages (WP). A summary of the most significant achievements for each WP is provided in the following:

*WP1: Bibliographic review on the influence of CO<sub>2</sub>, H<sub>2</sub> and N<sub>2</sub> in the evolution of the mechanical properties of the faults and the induced seismicity [1].* According to the scientific literature published at the date, the CO<sub>2</sub> seems to have negligible effects on the mechanical properties of faults while no quantitative assessment is documented about H<sub>2</sub> and N<sub>2</sub>. As a result, no geochemical effect was considered in the numerical model. Finally, a summary of the lessons learnt about induced seismicity is provided.

*WP2: Bibliographic review on the influence of CO<sub>2</sub>, H<sub>2</sub> and N<sub>2</sub> in the evolution of the mechanical properties of the rock and caprock [2].* The results of the laboratory tests are quite ambiguous, especially for sandstones: a  $\pm 30\%$  change in deformation moduli due to exposure to the CO<sub>2</sub> is observed. Regarding the effects of the H<sub>2</sub>, rock degradation has been observed but quantitative data are unavailable. The geochemical effects due to N<sub>2</sub> can be neglected because it is commonly used as a control gas. As a result, the following geochemical scenarios have been considered in the numerical model: weakening/hardening for the CO<sub>2</sub>, only weakening for H<sub>2</sub> and no geochemical effects for N<sub>2</sub>.

*WP3: Definition of the storage scenarios and dynamic simulations to compute the pore-pressure change [3].* The same geological and petrophysical configurations defined in KEM-01 project have been used. For each gas, two storage scenarios have been defined: an extreme scenario to account for short injection stages or high delta-pressure in storage cycles and a more realistic one in terms of injection/production rates. The results in terms of pore-pressure change in time and space are used in WP4 and WP5 for the set-up of the numerical model and the numerical analyses of the storage scenarios, respectively.

*WP4: Set-up of the numerical model [4].* The numerical approach is the combination of the reservoir model developed in WP3 and the geomechanical model. These two models are coupled together with the so-called one-way coupled approach: first, the pore-pressure change in space and time is

computed by the reservoir model, then, the pore-pressure change is used as external force in the geomechanical model. The geomechanical model uses the same geometrical configuration defined in KEM-01 project. The model is updated with a state-of-the-art numerical approach for the fault modeling and the hardening/weakening of the reservoir rock to take into account the geochemical effects of CO<sub>2</sub>, H<sub>2</sub> and N<sub>2</sub>. Finally, the numerical model is validated using several scenarios defined in KEM-01 project.

*WP5: Analysis with the numerical model [5].* First, different scenarios are defined for each gas. In particular, the same main configurations defined in KEM-01 are used: the geometries and mechanical parameters of the faults and reservoir are changed to investigate their effects compared to the reference case. The numerical model defined in WP4 is used to run the 3D geomechanical simulations. To facilitate the comparison with the results obtained in KEM-01 project, the model outcomes are presented in terms of the evolution over time of the maximum  $\chi = |\tau| / \tau_L$  (where  $\tau$  is the shear stress along the fault plane and  $\tau_L$  the shear stress limit defined through the Mohr-Coulomb criterion) which represents the main output of KEM-01 project.

*WP6: Definition of the guidelines.* The scenarios analyzed in WP5 are evaluated to define general rules: the numerical results for the CO<sub>2</sub>, H<sub>2</sub> and N<sub>2</sub> storage are comparable to that obtained in KEM-01 project for CH<sub>4</sub>. The geochemical effects, as considered in the numerical model, are negligible. As a conclusion, the same considerations made for Underground Gas Storage (UGS) still apply for CO<sub>2</sub>, H<sub>2</sub> and N<sub>2</sub> storage.

## Introduction

The evaluation of the numerical analyses performed in WP5 [5] are carried out in WP6 together with the definition of guidelines for a CO<sub>2</sub>, H<sub>2</sub> and N<sub>2</sub> safe storage. Safety is defined in terms of distance to fault reactivation during gas injection.

In the following, we refer to the steps listed below (Figure 1):

- Primary Production (PP): pressure decrease in the reservoir as a result of methane production;
- Storage (ST): pressure recovery in the reservoir due to the storage of CO<sub>2</sub> and N<sub>2</sub>;
- Cushion Gas (CG) injection: pressure recovery in the reservoir due to the cushion gas injection of H<sub>2</sub>;
- Underground H<sub>2</sub> Storage (UHS) cycles: seasonal pressure fluctuation in the reservoir as a result of the seasonal storage (UHS-S) and production (UHS-P) of H<sub>2</sub>;

The report is subdivided in the following sections: 1) comparison of numerical scenarios and ranking to evaluate the configurations most prone to fault reactivation; 2) final observations regarding KEM-39 project; 3) answers to the questions behind the KEM-39 project.

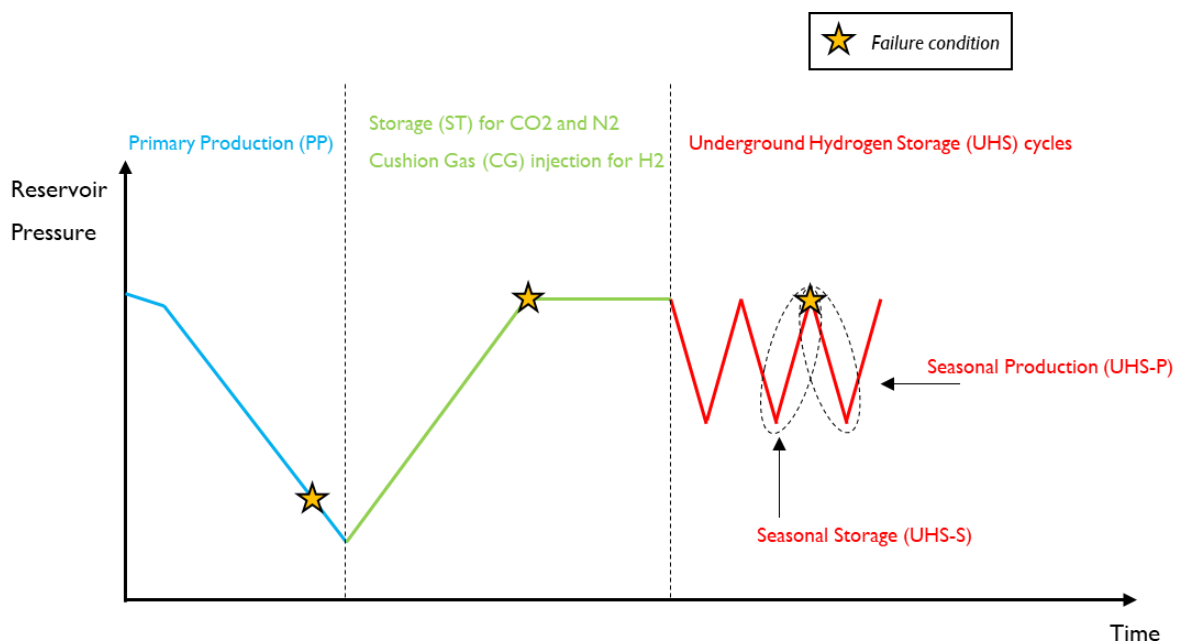


Figure 1: Sketch of the main stages during the reservoir lifespan in terms of pressure change over time.

## I Scenario Comparison

In this section all the scenarios analyzed in WP5 are compared using the  $t_{80}$  parameter. The  $t_{80}$  is defined as in KEM-I: the fault thickness with  $\chi$  value larger than 0.8 (i.e. the ration  $A_{80}/L$  where  $A_{80}$  is the fault area with  $\chi > 0.8$  and  $L$  is the fault length in the XY plane). Moreover, as done in KEM-I, the current analysis is focused on the two faults F3 and F2. The results are shown in Figure 2-Figure 3, Figure 4 to Figure 9, and Figure 10 to Figure 11 for CO<sub>2</sub>, H<sub>2</sub>, and N<sub>2</sub>, respectively.

From the comparison, the following observations can be made:

- The evolution over time of the parameter  $t_{80}$  is comparable of that of  $\chi$  maximum. First,  $t_{80}$  increases during PP due to the compaction and contraction of the reservoir: the former increases the shear stress along the fault while the latter unloads the normal stress decreasing the fault strength. The larger values are obtained in this primary stage. Then,  $t_{80}$  decreases at the beginning of the ST and CG stages because the shear stress along the fault is unloaded due to the expansion of the reservoir. Keeping up with the injection, if there was a fault reactivation during PP, the shear stress is loaded with opposite sign and  $t_{80}$  starts increasing.
- If a fault reactivates during the PP,  $t_{80}$  reaches a relative maximum at the end of the ST and CG stages. This maximum corresponds to the return of the pore-pressure in the reservoir to its initial value, before the beginning of the PP. Moreover, in the UHS cycles,  $t_{80}$  reaches relative maximum values at the end of the UHS-S stage (both Case I and Case 2) and at the end of the UHS-P stage (only Case I). These maximum values correspond to the highest and lowest value of the pressure in the reservoir, respectively.
- If a fault is not reactivation during the PP,  $t_{80}$  is kept at zero in the ST and CG stages and in the UHS cycles.
- During the PP, configuration C2 shows the maximum values of  $t_{80}$ : the reduction in friction angle plays a major role for the maximum  $t_{80}$ .
- During the ST and CG stages and in the UHS cycles, the four configurations C1, C2, C3 and C5 show comparable values in terms of maximum  $t_{80}$ : the reaching of the failure condition during the PP stage controls the maximum  $t_{80}$ , regardless of the geometrical and mechanical parameters of different configurations.

- The geochemical effects can be neglected. Only for storage Case I of the H2 (not realistic as pointed out in WP3[3]) the weakening increases the value of  $t_{80}$  at the end of the UHS-P stage, when the pressure in reservoir is at a relative minimum.

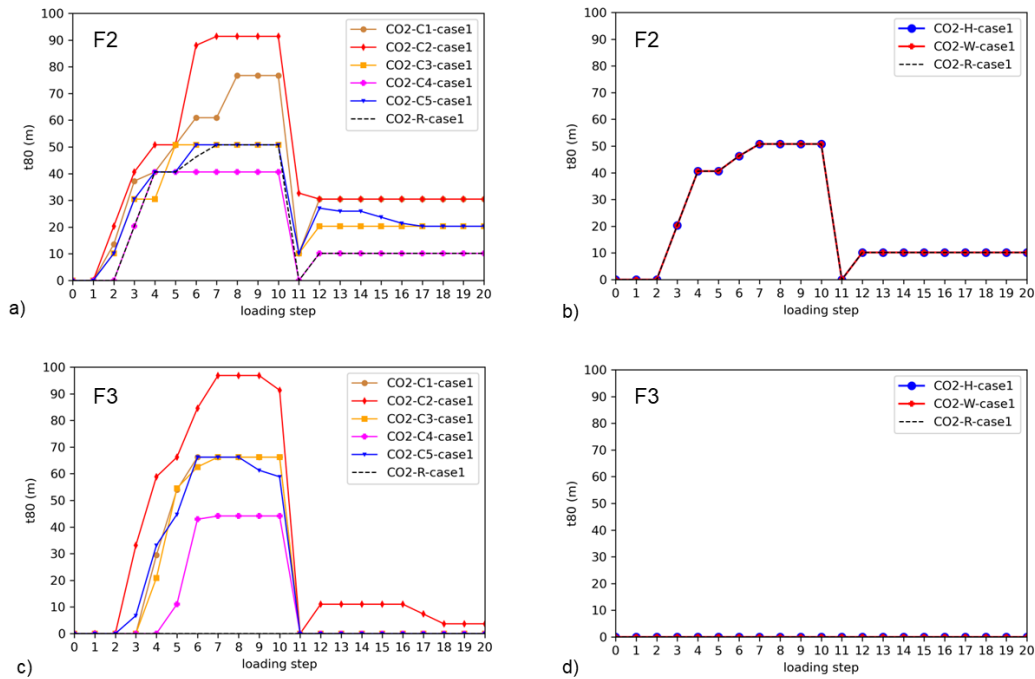


Figure 2: CO2 storage case 1 - Evolution in time of the parameter  $t_{80}$  (m) for the analyzed scenarios on fault F2 (a, b) and F3 (c, d).

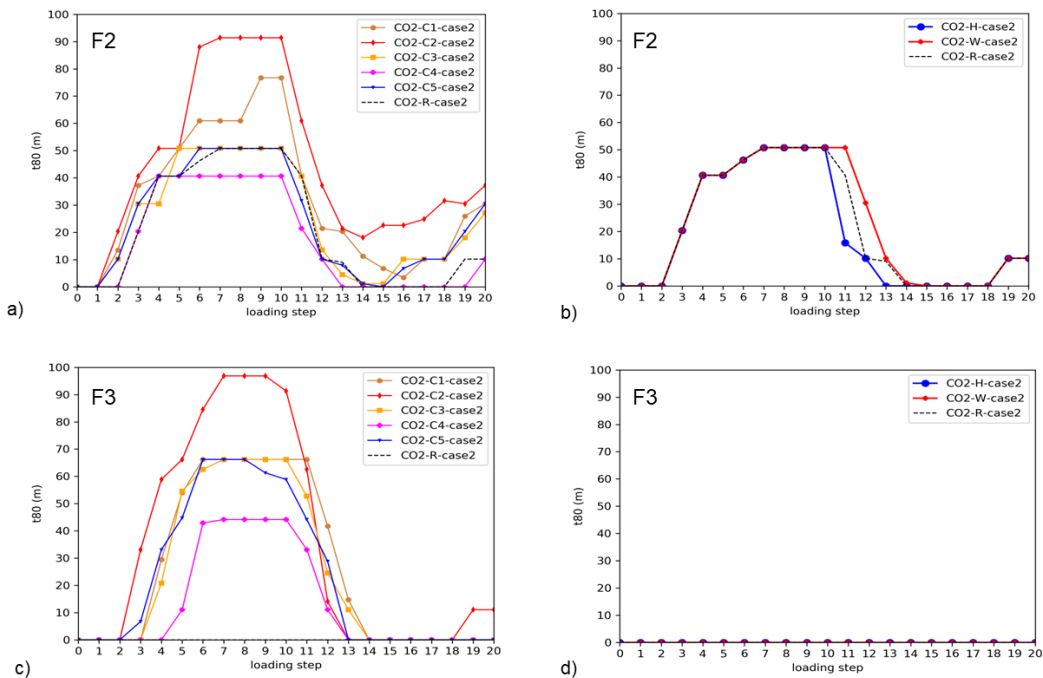


Figure 3: CO2 storage case 2 - Evolution in time of the parameter  $t_{80}$  (m) for the analyzed scenarios on fault F2 (a, b) and F3 (c, d).

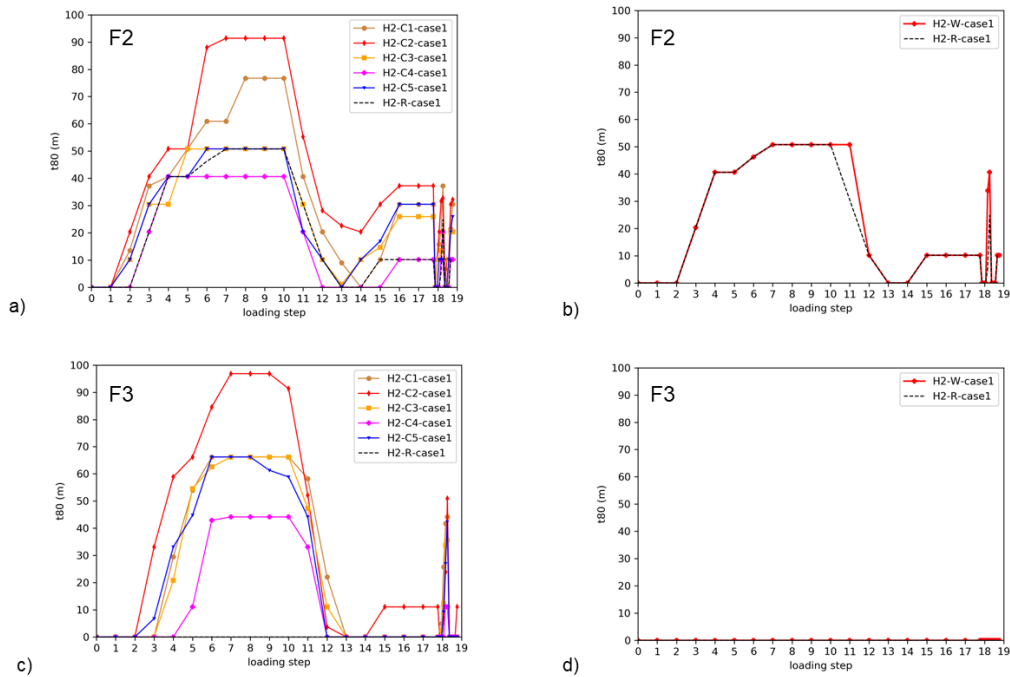


Figure 4: H2 storage case 1 - Evolution in time of the parameter  $t_{80}$  (m) for the analyzed scenarios on fault F2 (a, b) and F3 (c, d).

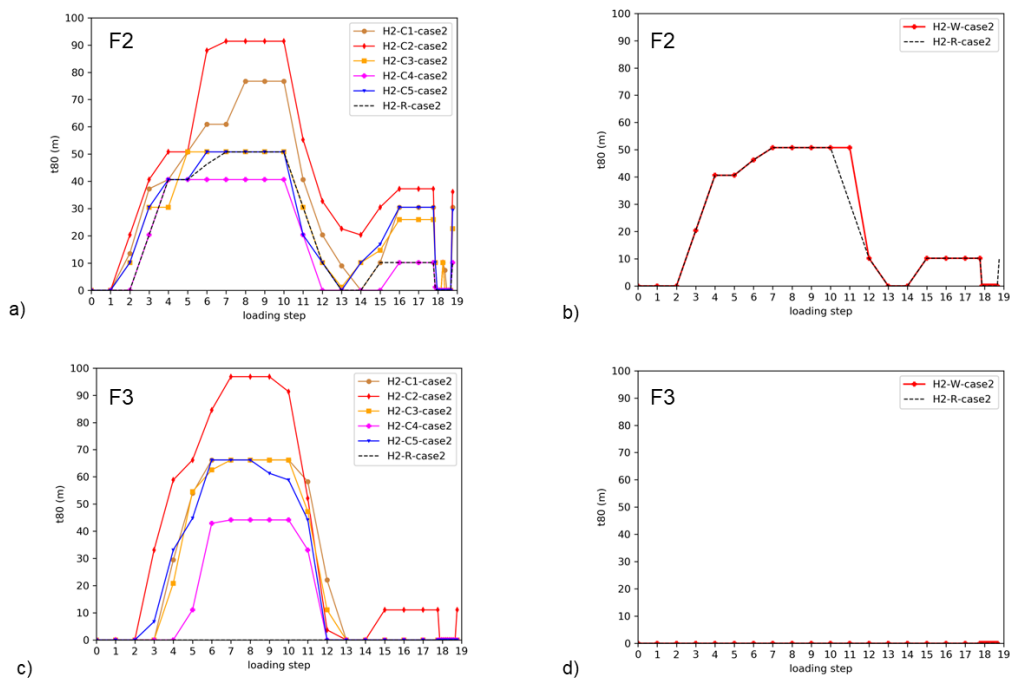


Figure 5: H2 storage case 2 - Evolution in time of the parameter  $t_{80}$  (m) for the analyzed scenarios on fault F2 (a, b) and F3 (c, d).

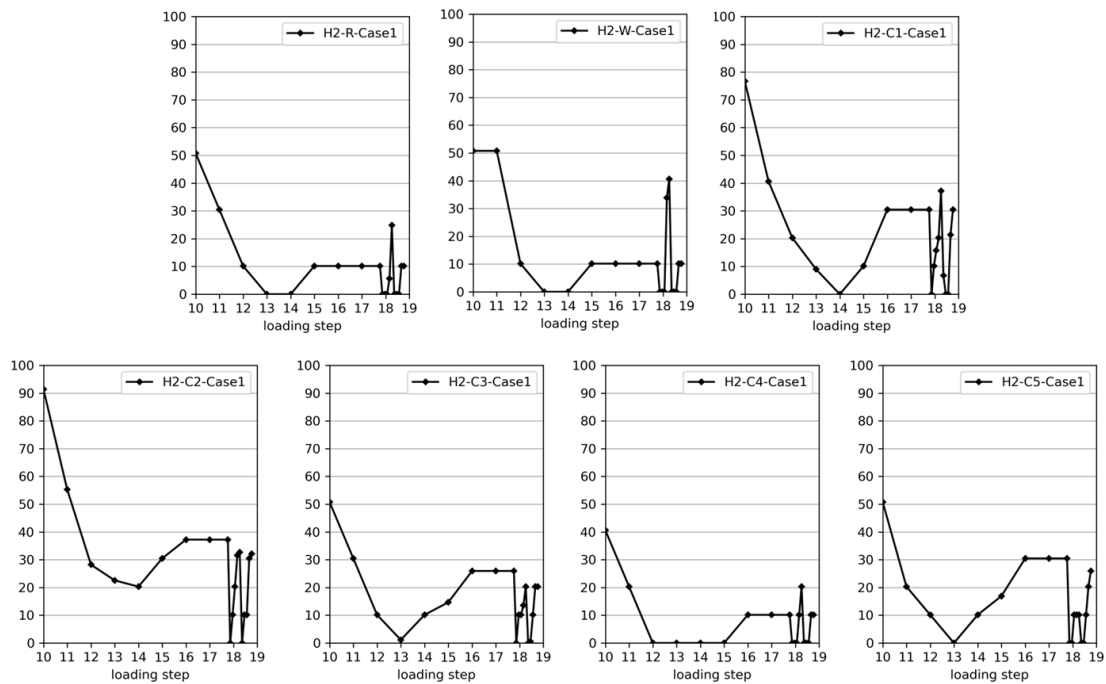


Figure 6: H2 storage case I - Evolution in time of the parameter  $t_{80}$  (m) for the analyzed scenarios on fault F2. The profiles refer only to the cushion gas injection and first storage cycle.

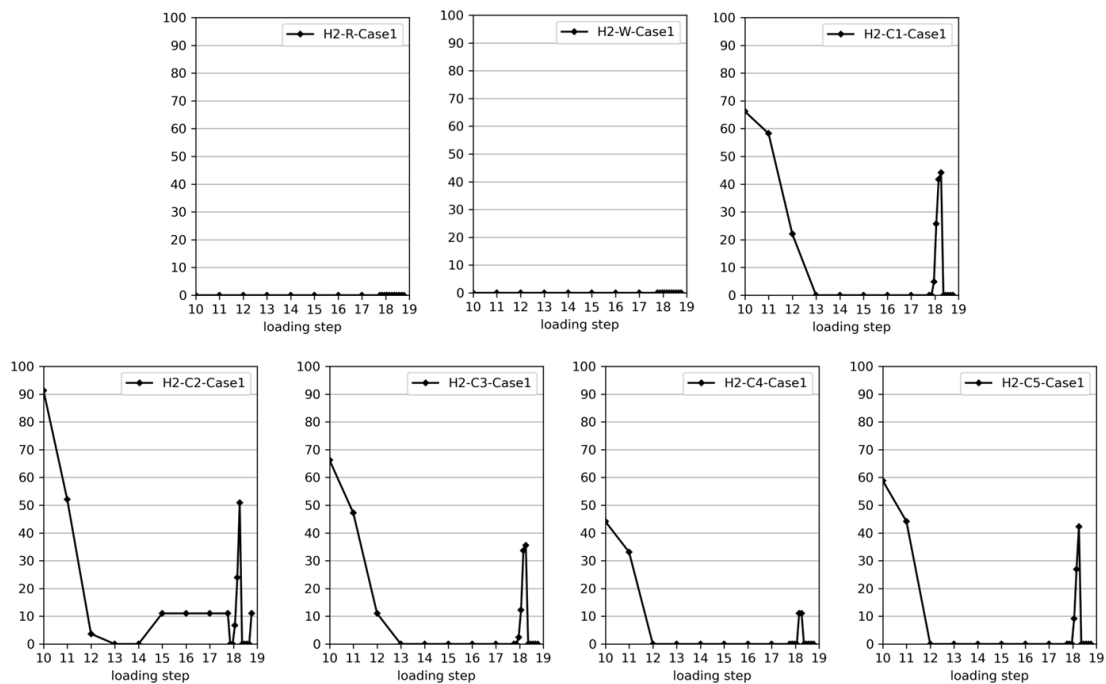


Figure 7: H2 storage case I - Evolution in time of the parameter  $t_{80}$  (m) for the analyzed scenarios on fault F3. The profiles refer only to the cushion gas injection and first storage cycle.

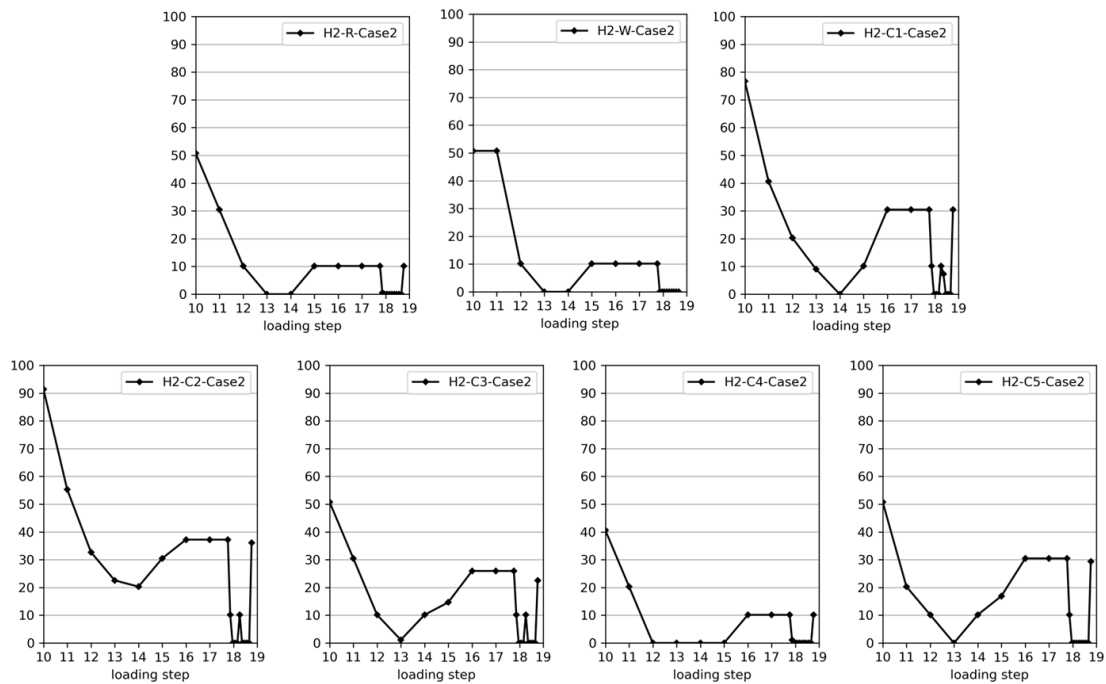


Figure 8: H2 storage case 2 - Evolution in time of the parameter  $t_{80}$  (m) for the analyzed scenarios on fault F2. The profiles refer only to the cushion gas injection and first storage cycle.

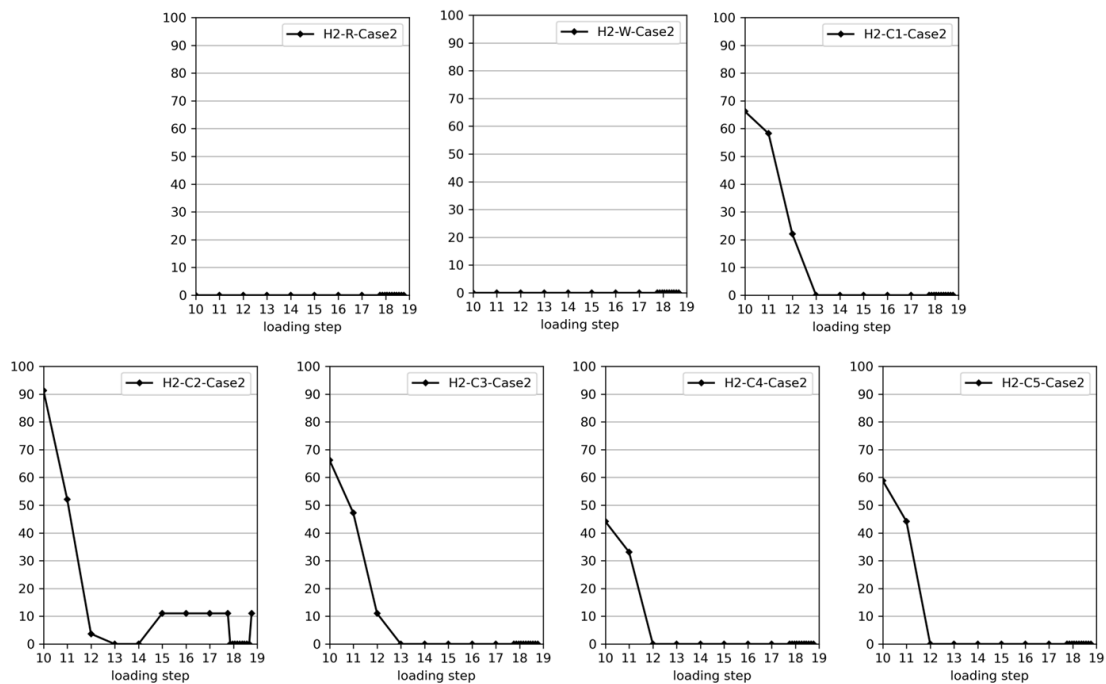


Figure 9: H2 storage case 2 - Evolution in time of the parameter  $t_{80}$  (m) for the analyzed scenarios on fault F3. The profiles refer only to the cushion gas injection and storage cases.

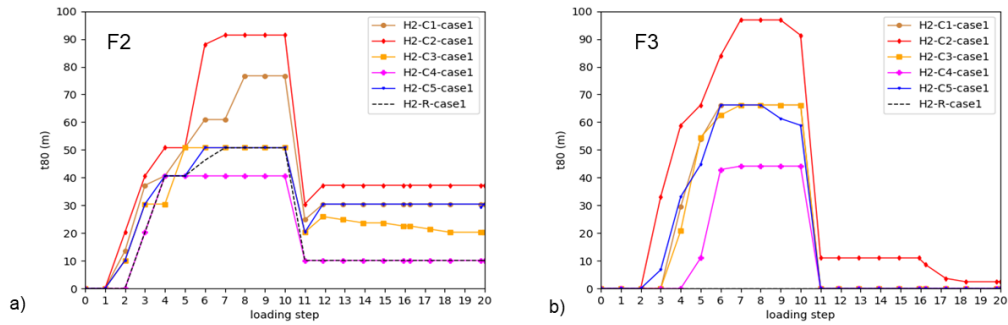


Figure 10: N2 storage case 1 - Evolution in time of the parameter  $t_{80}$  (m) for the analyzed scenarios on fault F2 (a) and F3 (b).

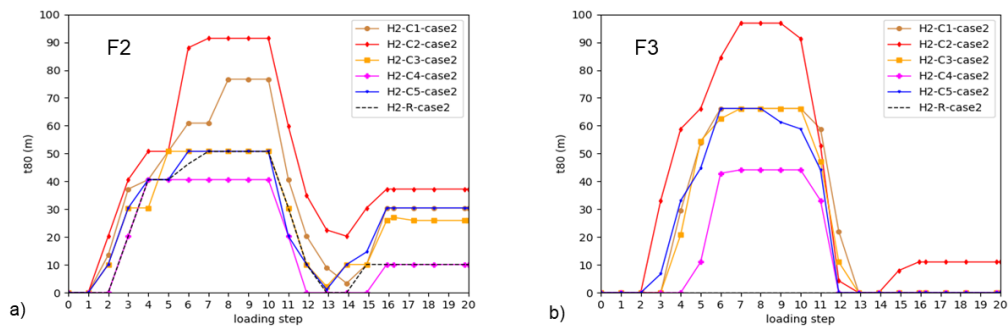


Figure 11: N2 storage case 2 - Evolution in time of the parameter  $t_{80}$  (m) for the analyzed scenarios on fault F2 (a) and F3 (b).

Finally, all the scenarios have been ranked following the nested criteria proposed in KEM-I [6]:

1.  $\chi$  maximum during the ST and CG stages and UHS cycles ( $\chi_{\max\text{STG}}$ );
2. maximum value of the fault sliding ( $\delta_{\max}$ );
3. loading step of activation (LS);

The results of the ranking procedure are reported in Table 1-Table 2, Table 3-Table 4 and Table 5-Table 6 for CO<sub>2</sub>, H<sub>2</sub> and N<sub>2</sub>, respectively. Again, the analysis focuses on the two faults, F3 and F2. Note that fault F3 is inactive in several scenarios because of symmetry in the reservoir compartments (no reservoir offset). As observed for the UGS, the scenarios more prone to activation during the PP are also the most critical ones during ST and CG stages and UHS cycles.

Table 1: CO<sub>2</sub> storage: ranking of the analyzed scenarios, from the most to the least prone to induce reactivation of fault F2.

	Scenario	$\chi_{\max\text{STG}}$	$\delta_{\max}$	LS	$\chi_{\max}$
Fault F2	CO2-C1-Case1	0.85	0.005	6	1.00
	CO2-C2-Case1	0.84	0.010	5	1.00
	CO2-C1-Case2	0.84	0.006	6	1.00
	CO2-R-Case1	0.82	0.004	10	0.99
	CO2-C2-Case2	0.81	0.010	5	1.00
	CO2-H-Case2	0.81	0.004	10	0.99
	CO2-W-Case1	0.81	0.004	10	0.99
	CO2-H-Case1	0.80	0.004	10	0.99
	CO2-C5-Case1	0.79	0.004	6	1.00
	CO2-R-Case2	0.79	0.004	10	0.99
	CO2-W-Case2	0.78	0.004	10	0.99
	CO2-C5-Case2	0.77	0.004	6	1.00
	CO2-C3-Case2	0.74	0.008	6	1.00
	CO2-C3-Case1	0.72	0.008	6	1.00
	CO2-C4-Case2	0.69	0.003	-	0.88
	CO2-C4-Case1	0.66	0.003	-	0.88

Table 2: CO<sub>2</sub> storage: ranking of the analyzed scenarios, from the most to the least prone to induce reactivation of fault F3.

	Scenario	$\chi_{\max}$ STG	$\delta_{\max}$	LS	$\chi_{\max}$
Fault F3	CO2-C2-Case2	0.66	0.003	-	0.94
	CO2-C2-Case1	0.60	0.003	-	0.94
	CO2-C5-Case2	0.46	0.001	-	0.81
	CO2-C3-Case2	0.37	0.001	-	0.71
	CO2-C5-Case1	0.36	0.001	-	0.81
	CO2-C1-Case1	0.31	0.001	-	0.75
	CO2-C1-Case2	0.29	0.001	-	0.74
	CO2-C3-Case1	0.29	0.001	-	0.71
	CO2-C4-Case1	0.25	0.000	-	0.64
	CO2-C4-Case2	0.24	0.000	-	0.64
	CO2-R-Case1	0.00	0.000	-	0.00
	CO2-W-Case1	0.00	0.000	-	0.00
	CO2-H-Case1	0.00	0.000	-	0.00
	CO2-R-Case2	0.00	0.000	-	0.00
	CO2-W-Case2	0.00	0.000	-	0.00
	CO2-H-Case2	0.00	0.000	-	0.00

Table 3: H<sub>2</sub> storage: ranking of the analyzed scenarios, from the most to the least prone to induce reactivation of fault F2.

	Scenario	$\chi_{\max}$ STG	$\delta_{\max}$	LS	$\chi_{\max}$
Fault F2	H2-C2-Case1	0.92	0.010	5	1.00
	H2-W-Case1	0.88	0.004	10	0.99
	H2-C1-Case1	0.87	0.005	6	1.00
	H2-C3-Case1	0.84	0.008	6	1.00
	H2-C1-Case2	0.84	0.005	6	1.00
	H2-C5-Case1	0.84	0.004	6	1.00
	H2-C2-Case2	0.82	0.010	5	1.00
	H2-R-Case1	0.77	0.004	10	0.99
	H2-R-Case2	0.77	0.004	10	0.99
	H2-C5-Case2	0.76	0.004	6	1.00
	H2-W-Case2	0.76	0.004	10	0.99
	H2-C3-Case2	0.74	0.008	6	1.00
	H2-C4-Case1	0.71	0.003	-	0.88
	H2-C4-Case2	0.71	0.003	-	0.88

Table 4: H2 storage: ranking of the analyzed scenarios, from the most to the least prone to induce reactivation of fault F3.

	Scenario	$\chi_{\max}$ STG	$\delta_{\max}$	LS	$\chi_{\max}$
Fault F3	H2-C2-Case1	0.81	0.003	-	0.94
	H2-C5-Case1	0.71	0.001	-	0.81
	H2-C1-Case1	0.67	0.001	-	0.75
	H2-C2-Case2	0.65	0.003	-	0.94
	H2-C3-Case1	0.64	0.001	-	0.70
	H2-C5-Case2	0.59	0.001	-	0.81
	H2-C4-Case1	0.57	0.001	-	0.75
	H2-C4-Case1	0.57	0.000	-	0.63
	H2-C3-Case2	0.55	0.001	-	0.70
	H2-C4-Case2	0.48	0.000	-	0.64
	H2-R-Case1	0.00	0.000	-	0.00
	H2-W-Case1	0.00	0.000	-	0.00
	H2-R-Case2	0.00	0.000	-	0.00
	H2-W-Case2	0.00	0.000	-	0.00

Table 5: N2 storage: ranking of the analyzed scenarios, from the most to the least prone to induce reactivation of fault F2.

	Scenario	$\chi_{\max}$ STG	$\delta_{\max}$	LS	$\chi_{\max}$
Fault F2	N2-C1-Case1	0.85	0.005	6	1.00
	N2-C1-Case2	0.84	0.005	6	1.00
	N2-C2-Case2	0.80	0.010	5	1.00
	N2-C2-Case1	0.79	0.010	5	1.00
	N2-R-Case2	0.78	0.004	10	0.99
	N2-R-Case1	0.77	0.004	10	0.99
	N2-C3-Case2	0.76	0.008	6	1.00
	N2-C5-Case2	0.76	0.004	6	1.00
	N2-C5-Case1	0.75	0.004	6	1.00
	N2-C3-Case1	0.73	0.008	6	1.00
	N2-C4-Case1	0.71	0.003	-	0.88
	N2-C4-Case2	0.71	0.003	-	0.88

Table 6: N2 storage: ranking of the analyzed scenarios, from the most to the least prone to induce reactivation of fault F3.

	Scenario	$\chi_{\max}$ STG	$\delta_{\max}$	LS	$\chi_{\max}$
Fault F3	N2-C2-Case1	0.64	0.003	-	0.94
	N2-C2-Case2	0.63	0.003	-	0.94
	N2-C5-Case2	0.44	0.000	-	0.81
	N2-C5-Case1	0.39	0.001	-	0.81
	N2-C3-Case2	0.36	0.001	-	0.71
	N2-C3-Case1	0.32	0.001	-	0.71
	N2-C1-Case2	0.28	0.001	-	0.75
	N2-C1-Case1	0.27	0.001	-	0.75
	N2-C4-Case2	0.22	0.000	-	0.64
	N2-C4-Case1	0.22	0.000	-	0.64
	N2-R-Case1	0.00	0.000	-	0.00
	N2-R-Case2	0.00	0.000	-	0.00

## 2 Final observations

The evaluation of the scenarios analyzed in this project leads to the conclusion that the considerations made in KEM-I for UGS of CH<sub>4</sub> are still valid for CO<sub>2</sub>, H<sub>2</sub> and N<sub>2</sub> storage. In particular, it has been observed that reactivation of faults, or a stress-state close to failure, occurs during the ST and CG stages and UHS cycles when (Figure 1):

- faults reached failure during the primary production phase;
- the pressure in the reservoir at the end of the injection stage is close to the initial value (before primary production);
- the pressure in the reservoir during the UHS cycles is close to the initial value (before primary production);

Moreover, the single fault reactivation is case-sensitive: it depends on the geometry and mechanical properties of the fault, reservoir, and surrounding formations.

As a result, the same guidelines defined in KEM-I [6] are still valid for the CO<sub>2</sub>, H<sub>2</sub> and N<sub>2</sub> storage in depleted gas fields.

The authors emphasize that these general guidelines are only qualitative due to the nature of numerical analysis: the modeling framework consists of realistic but synthetic test cases. However, they can be considered conservative in that they aim to avoid or limiting fault failure (reactivation, in fact, can occur with aseismic slip).

A final note regarding geochemical effects on fault and rock mechanical properties due to CO<sub>2</sub>, H<sub>2</sub>, N<sub>2</sub> exposure: as considered in the numerical model, these effects are negligible. However, the authors point out a lack of laboratory testing and consequently a challenge in collecting quantitative information to be use in the modeling.

### 3 Answers to the questions behind the KEM-39 project

The project is aimed at answering the following questions:

1. Which main factors control the reactivation of faults and seismicity under permanent or cyclic storage conditions of CO<sub>2</sub>, H<sub>2</sub>, N<sub>2</sub>?
2. To which extent is the formation pressure affected differently for the different types of storage fluid?
3. To which extent can geochemical dissolution effects cause mechanical weakening of the reservoir or faults in the caprock?
4. To which extent are the mechanisms for seismicity similar to the mechanisms during natural gas storage?
5. Relate to the existing conclusions of KEM-01. Which conclusions still stand for gasses other than natural gas (CO<sub>2</sub>, H<sub>2</sub>, N<sub>2</sub>)? Which conclusions change?

Taking into account the limitations of the present study (lack of laboratory data and qualitative numerical analysis), described in detail in WP1-WP5 reports and summarized in the previous sections, the following answers can be derived:

1. Fault reactivation (which can be aseismic) occurs when: (1) faults reached failure during the primary production phase; (2) the pressure in the reservoir at the end of the injection stage is close to the initial value (before primary production); (3) the pressure in the reservoir during the UHS cycles is close to the initial value (before primary production);
2. Depending on the type of fluid, the injection can have different purposes: sequestration (for CO<sub>2</sub> and N<sub>2</sub>) or storage cycles (for H<sub>2</sub>). With the former, the pressure history consists only of an injection phase; the latter also has seasonal cycles of injection/production. In addition, the injection phase may have a different time span.
3. There is a lack of quantitative data regarding the effects of N<sub>2</sub> and H<sub>2</sub>. Regarding CO<sub>2</sub>: the effects on mechanical properties of faults are negligible; both weakening and hardening effects have been observed on reservoir and caprock with a  $\pm 30\%$  change in deformation moduli.
4. The geochemical effects are negligible (as they were accounted for in the numerical model) and fault critical conditions are controlled by the extreme values of pore-pressure (minimum and maximum) in the formation. Since these values are similar for the natural gas storage operations, the mechanisms for reactivation (which can be aseismic) are also similar.
5. All the conclusions of KEM-01 stand for CO<sub>2</sub>, H<sub>2</sub> and N<sub>2</sub>.

## References

1. M3E. *Study within the Mining Effects Knowledge Program (KEM-39) on the cyclic storage of gases in the Netherlands – WP1*. Technical Report, 2022.
2. M3E. *Study within the Mining Effects Knowledge Program (KEM-39) on the cyclic storage of gases in the Netherlands – WP2*. Technical Report, 2022.
3. M3E. *Study within the Mining Effects Knowledge Program (KEM-39) on the cyclic storage of gases in the Netherlands – WP3*. Technical Report, 2022.
4. M3E. *Study within the Mining Effects Knowledge Program (KEM-39) on the cyclic storage of gases in the Netherlands – WP4*. Technical Report, 2022.
5. M3E. *Study within the Mining Effects Knowledge Program (KEM-39) on the cyclic storage of gases in the Netherlands – WP5*. Technical Report, 2022.
6. DICEA, University of Padova. *KEM-01: Safe Operational Bandwidth of Gas Storage Reservoirs – WP7*. Technical Report, 2019.